A Hierarchical Consensus Based Negotiation Scheme for Multi-platoon Cooperative Control

Jiayu Cao, Supeng Leng, *Member, IEEE,* Jianhua He, *Senior Member, IEEE,* and Hanwen Zhang

***Abstract*—Cooperative platooning holds great potential for driving safety and road efficiency. However, limited communication resources and dynamic network topologies pose challenges to reliable and timely vehicular negotiation on joint platoon control (e.g., changing lanes and giving ways) in cooperative platooning. In this article, we propose a new hierarchical consensus framework to support reliable and fast coordination among multiple platoons for safe and efficient driving control. The hierarchical consensus framework consists of intra-platoon and inter-platoon schemes. For the intra-platoon scheme, we propose a new Practical Byzantine Fault Tolerance (PBFT) enabled intra-platoon consensus mechanism. An adaptive local consensus scheme is designed to reduce the local consensus delay and improve the successful local consensus ratio. For the inter-platoon consensus, we develop a new Raft and 5G Time Sensitive Networking (5G-TSN) based scheme to enhance the responsiveness and scalability of multi-platoon negotiations. Furthermore, we design a dynamic prioritization scheme for 5G-TSN flows and develop an intelligent flow scheduling algorithm to improve interactions among platoons and shorten the total negotiation delay, while ensuring successful multi-platoon negotiations. Simulation results indicate that the proposed scheme can significantly enhance the multi-platoon negotiation performance for cooperative control, with more than 16.9% higher successful consensus ratio and 14% lower negotiation delay than existing approaches.**

***Index Terms*—Platoon, autonomous driving, distributed consensus, 5th Generation Time Sensitive Networking (5G-TSN).**

I. Introduction

With the increase of urbanization and vehicle ownership, the global road transport system is facing big challenges. More than 1 million people lost their lives on roads every year. Road transport system is also a major contributor to the carbon dioxide emission. Connected Autonomous Driving (CAD) is widely viewed as a promising technology to tackle road transport challenges. In the 5th Generation (5G) vehicle-to-everything (V2X) specifications, four CAD advanced use cases were specified, which include cooperative sensing, remote driving, platooning, and cooperative driving. For the platooning scenario, vehicles can communicate via V2X and cooperatively drive in a platoon with reduced inter-vehicle distance and improved perception, which can largely enhance road and fuel efficiency, and reduce accidents [1]. There have been strong research and industry interests in cooperative platooning for road safety and efficiency. Field trials of platoons are already conducted on highways in many countries [2] [3].

The existing research work mainly focuses on platoon-based autonomous driving control. However, for multiple platoons intending to reorganize, stagger, reroute, or make way for other platoons, any conflicting decisions or misbehavior can impede the rapid response of platoons and lead to potential accidents [4]–[6]. Consequently, multi-platoon negotiation is critical for coordinated platoon control within and among platoons. Nevertheless, it is very challenging to achieve multi-platoon negotiation in a dynamic environment with a large number of participants and limited communication resources. Although current 5G vehicle-to-vehicle (V2V) communications facilitate real-time interaction within platoons [7]–[9], negotiating among platoons over long communication distances (requiring multi-hop relays) and associated unaffiliated vehicles is still difficult. As a result, the prolonged interaction among multiple platoons delays and fails the negotiation on critical cooperative platoon driving decisions. In addition, the potential non-responsive or incorrectly perceived vehicles within platoons, due to unsuccessful activation of negotiation programs or constrained perception conditions, can further hinder the success of multi-platoon negotiations. Thus, it is imperative to design a robust, reliable, and timely negotiation scheme for platoons to consult and agree on coordinated multi-platoon driving control.

This article is motivated to address the challenges of multi-platoon negotiation in dynamic and resource-constrained environments. Distributed consensus is considered a pivotal technology to solve the negotiation issue among vehicles [10]–[12]. Vehicles can negotiate efficiently with distributed consensus protocols, such as the Raft protocol [13] and the Practical Byzantine Fault Tolerance (PBFT) protocol [14]. However, existing Raft-based approaches are insufficient to deal with negotiation scenarios involving Byzantine errors (i.e., potentially non-responsive vehicles and possibly incorrect vehicular perception). PBFT-based solutions are fault-tolerant, but their deployment is restricted to fixed and small-scale applications [10]. In addition, traditional consensus mecha-

This work was partly supported by National Natural Science Foundation of China (No. 62171104), Chengdu Bureau of Science and Technology with No. 2023-YF06-00030-HZ, EPSRC with RC Grant No. EP/Y027787/1, and UKRI under grant No. EP/Y028317/1. *(Corresponding author: Supeng Leng.)*

Jiayu Cao and Hanwen Zhang are with the school of Information and Communication Engineering, University of Electronic Science and Technology of China, Chengdu 611731, China, (e-mail: liuda945@163.com; margaret_zhw@foxmail.com).

Supeng Leng is with the school of Information and Communication Engineering, University of Electronic Science and Technology of China, Chengdu 611731, China, and also with the Shenzhen Institute for Advanced Study, UESTC, Shenzhen, China, (e-mail: spleng@uestc.edu.cn).

Jianhua He is with the School of Computer Science and Electronic Engineering, University of Essex, CO4 3SQ Colchester, U.K, (e-mail: j.he@essex.ac.uk).

nisms for wired communication networks are still unsuitable for vehicular networks with dynamic topologies. Meanwhile, current wireless link based solutions may cause long and uncertain negotiation delays in multi-platoon scenarios, as well as low successful consensus ratios [15].

In this article, we propose a new Hierarchical Consensus empowered Vehicular Negotiation (HCVN) scheme aimed at fast and reliable coordination for multi-platoon cooperative control. Leveraging layered and parallel consensus techniques, we develop a hierarchical consensus framework that integrates PBFT and Raft protocols, containing multiple PBFT-enabled intra-platoon consensuses and one Raft-enabled inter-platoon consensus. Furthermore, multi-channel V2V communication and 5G Time Sensitive Networking (5G-TSN) technologies [16] are incorporated into intra-platoon and inter-platoon consensuses, respectively. Specifically, we devise optimal consensus schemes for intra-platoon and inter-platoon, respectively, to ensure successful multi-platoon negotiations and minimize the total negotiation delay with resource constraints and potential vehicle errors. Simulation results show that our proposed scheme can improve the coordination of multi-platoon cooperative control in various scenarios with low negotiation delay. The main contributions are listed as follows.

- We propose a new hierarchical consensus framework for multi-platoon negotiation, aiming to solve the issues of low successful consensus ratios and inadequate real-time performance in existing solutions and support the close coordination of multi-platoon cooperative control. In the hierarchical framework, the PBFT protocol is exploited for intra-platoon consensus to attain a high local successful consensus ratio even with potentially non-responsive vehicles and possibly low-quality perception. The Raft protocol is adopted for inter-platoon consensus, which can simplify the interaction among platoons and enhance the time-sensitivity and scalability of multi-platoon negotiations.
- We present a new intra-platoon consensus mechanism with a 3-phase dynamic negotiation interaction. Unlike existing approaches, we integrate multi-channel V2V into PBFT to accelerate the intra-platoon consensus process. We derive the successful consensus ratio within the platoon and conduct a theoretical analysis of the local negotiation delay. Building upon these analyses, a sub-gradient based intra-platoon consensus scheme is designed to minimize the local negotiation delay while ensuring a high local successful consensus ratio by adaptively adjusting the interaction time slot length and channel allocation.
- Based on the intra-platoon consensus, we propose a new Raft and 5G-TSN enabled inter-platoon consensus mechanism to promote the responsiveness and successful consensus ratio of inter-platoon negotiation. On the one hand, the 5G-TSN technology is applied to guarantee the real-time transmission of single consensus messages among platoons. On the other hand, a dynamic prioritization scheme and a Deep Deterministic Policy Gradient (DDPG) based scheduling algorithm are formulated for 5G-TSN flows to optimize the interaction of inter-platoon consensus, reduce the total negotiation delay, and improve the coordination of multi-platoon cooperative control.

The rest of the paper is organized as follows. In Section II, we review related work. We introduce the system model in Section III and propose a PBFT and V2V empowered intra-platoon consensus scheme in Section IV. The Raft and 5G-TSN enabled inter-platoon consensus is developed in Section V. We present simulation results in Section VI. Finally, Section VII concludes this article.

II. RELATED WORK

As the demand for traffic automation and enhanced travel safety continues to rise, cooperative platooning is anticipated to gain widespread acceptance. In [17], the authors developed a platooning protocol to facilitate the formation of long-body heavy-duty trucks. In [18], the authors proposed a hybrid approach for efficiently establishing and sustaining platoons. In [19], the authors explored the impact of various autonomous vehicle formations on traffic performance. C. Chen *et al*. [20] offered a method for making optimal insertion point decisions to group vehicles into a platoon. Nevertheless, a significant portion of prior research solely addresses the collaborative management of individual platoons, while overlooking the coordination among multiple platoons.

To enhance the safety of platoon driving, the consensus mechanism has been leveraged in the vehicular negotiation. In [21], the authors proposed a cooperation framework based on the PBFT protocol to improve the safety of autonomous driving applications. In [22], the authors explored the application of PBFT and Raft in connected critical autonomous systems. H. Seo *et al*. [23] designed a novel distributed consensus protocol to ensure the reliability of mission-critical decision-making in autonomous driving systems. However, existing solutions are primarily tailored for small-scale scenarios with simple communications and may cause excessive latency in driving applications that require multi-platoon negotiation and involve complex communications.

The 3rd Generation Partnership Project (3GPP) introduces TSN support for the 5G Radio Access Network (RAN) in Release 17 [16]. In the 5G-TSN framework, the 5G System (5GS) is embedded in TSN as a logic bridge and interacts with TSN by using TSN translators installed on the 5GS device side and network side, which enables the time-sensitive communication among platoons. Regarding time synchronization within the 5G-TSN framework, the TSN translators in the 5GS will update the residence time inside the 5GS to the TSN. Consequently, the 5GS no longer needs to be synchronized with the TSN grandmaster time. Nonetheless, 5G-TSN remains a nascent technology and research on its applications is still relatively limited.

In [24], the authors offered a comprehensive overview of the 5G integration with TSN and introduced a range of potential use cases that can benefit from 5G-TSN. In [25], the authors delved into the application of 5G-TSN in typical industrial use cases. In [26], the authors focused on the end-to-end latency performance of 5G-TSN systems. In [27], the authors designed an edge-assisted 5G-TSN architecture for the

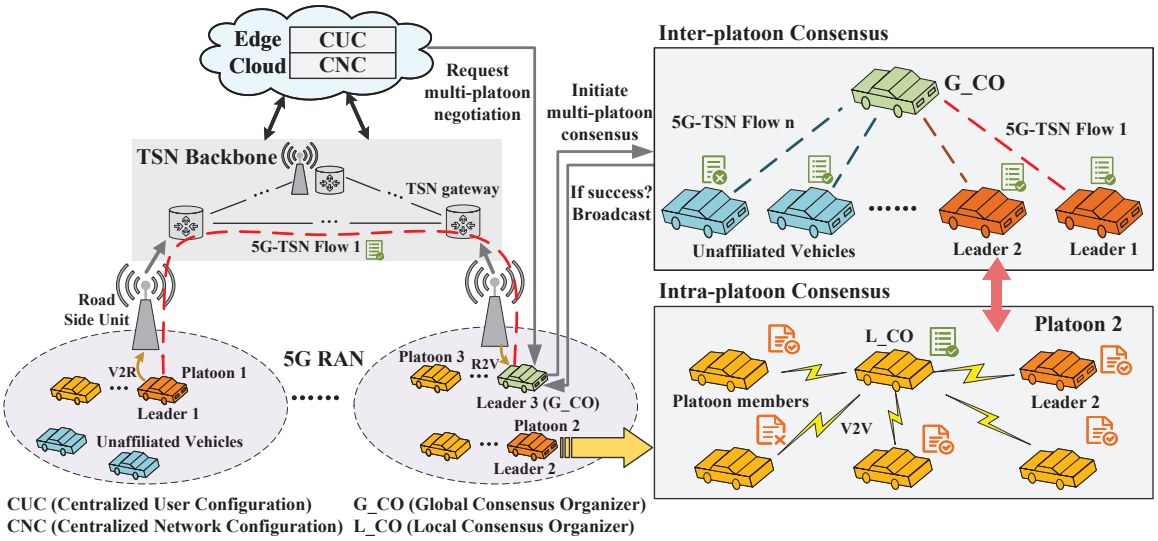

Fig. 1. The HCVN scheme for multi-platoon cooperative control.

Industrial Internet of Things. D. Wang *et al*. [28] discussed the role of 5G-TSN in supporting cloud vehicles. Although these works have provided valuable insights into the application of 5G-TSN, the integration of 5G-TSN with multi-platoon cooperative control has not been thoroughly studied.

Based on the above observations, coordinated platoon control depends on efficient negotiation among related vehicles. However, existing vehicular negotiation schemes lead to excessive delays and low successful consensus ratios in multi-platoon scenarios. Furthermore, while 5G-TSN presents a potential solution for rapid inter-platoon interactions, its application in multi-platoon negotiations is still unexplored.

III. SYSTEM MODEL

In multi-platoon scenarios such as emergency rescue, logistics, etc., cooperative control among multiple platoons requires negotiation and approval from all vehicles involved. Therefore, we propose an HCVN scheme to achieve fast and successful negotiation among multiple platoons and promote the coordination of multi-platoon cooperative control. In this section, we introduce the system model and basic assumptions.

A. System Overview

Fig. 1 shows our proposed HCVN scheme. M Road Side Units (RSUs) are distributed along the road. Each RSU is equipped with a TSN gateway (GW). Within the coverage area of the m-th RSU, K_m platoons and V_m unaffiliated vehicles not belonging to either platoon are driving on the road. N_k is the number of vehicles in the k-th platoon. Each vehicle is equipped with an onboard unit that can cache, calculate, and communicate with others in proximity via V2V communication. To reduce the negotiation delay among multiple platoons, we employ hierarchical and parallel negotiation techniques. Multi-platoon negotiation is divided into multiple local intra-platoon consensus and one global inter-platoon consensus. In the intra-platoon consensus, the Local Consensus Organizer (L_CO) organizes the vehicles in the same convoy to complete consensus with the assistance of V2V communication. In the inter-platoon consensus, the participants include the leaders of each platoon and all relevant unaffiliated vehicles. They will perform consensus under the guidance of the Global Consensus Organizer (G_CO). Moreover, to alleviate the impact of inter-platoon communication that requires multi-hop relaying or cross RSUs on the consensus delay, 5G-TSN communication is leveraged in the inter-platoon consensus to enhance the response speed.

In the HCVN scheme, a request for multi-platoon negotiation will be dispatched to the G_CO when the centralized control unit in the edge cloud makes critical decisions such as reorganizing, staggering, rerouting, or giving way. Critical control decisions will be used as the consensus content of the multi-platoon negotiation. Next, following the proposed Raft-based inter-platoon consensus mechanism, the G_CO will multicast the multi-platoon consensus content to the leaders and all relevant unaffiliated vehicles. Upon receiving the consensus file, the leaders will send an intra-platoon consensus request to the L_CO within their respective platoons. Subsequently, each L_CO will initiate the local consensus based on our proposed PBFT-based intra-platoon consensus mechanism. Simultaneously, unaffiliated vehicles will verify the multi-platoon consensus using their own perceptions. Once the intra-platoon consensus or verification of unaffiliated vehicles is accomplished, the leaders and unaffiliated vehicles will report the outcome (yes/no) to the G_CO. Then, the G_CO can judge whether the multi-platoon consensus is successful according to the proposed inter-platoon consensus mechanism. If successful, it indicates that the corresponding critical decision is coordinated, and the G_CO will notify all relevant platoons and vehicles to execute the decision via 5G-TSN broadcast communication. Otherwise, the G_CO will reorganize the consensus, or the critical decision will be remade by the centralized control unit.

The consensus process outlined above constitutes the

essence of multi-platoon negotiations. Its performance is directly linked to the applicability of our proposed scheme in time-sensitive multi-platoon cooperative driving systems. Consensus protocol selection and communication design are the crux of the consensus process. An unsuitable consensus protocol may result in vehicles failing to reach a consensus, while inappropriate communication designs can postpone the consensus process, thus affecting the overall consensus delay and successful consensus ratio. Hence, this article mainly focuses on the protocol selection and communication design of the consensus process. Detailed communication and consensus models are formulated in this section.

B. Communication Model

5G-TSN communications are utilized for negotiation interactions among leaders as well as between leaders and unaffiliated vehicles. 3GPP Release 17 elucidates the fundamental functionalities and architecture of 5G-TSN technology [16]. In this framework, the 5GS is seamlessly integrated into the TSN network, serving as a logical bridge to facilitate time-sensitive communication with end devices. As illustrated in Fig. 1, each TSN GW is outfitted with a 5G interface and can communicate with leader vehicles and unaffiliated vehicles via 5G technology. In this context, each interaction between any two vehicles constitutes a 5G-TSN flow. The i-th 5G-TSN flow f_i can be indicated as $f_i = \{So_{f_i}, De_{f_i}, S_{f_i}\}$, where So_{f_i} represents the source vehicle of f_i, De_{f_i} is the destination vehicle of f_i, and S_{f_i} is the packet size of f_i. Since the scheduling and configuration of 5G-TSN flows necessitate centralized computing, we adopt the fully centralized architecture specified in the IEEE 802.1Qcc standard. This architecture includes a Centralized User Configuration (CUC) module and a Centralized Network Configuration (CNC) module, as detailed in [16] and [25].

Furthermore, 5G New Radio (NR) air interface empowered V2V communication is adopted for the intra-platoon information interactions, which supports multiple communication modes, including unicast, multicast, and broadcast [7]. Assume that B is the bandwidth of V2V communication and is divided into G channels. The transmission rate of the l-th V2V link on the g-th channel is $r_{l,g} = B/G \log\left(1 + SINR_{l,g}\right)$. $SINR_{l,g}$ is the signal-to-interference-plus-noise rate (SINR) of the l-th V2V link with the g-th channel. Suppose the unit price of the V2V channel per unit time is c_{v2v}. Therefore, the cost of the l-th V2V link transmitting the consensus files on the g-th channel can be expressed as $o_{l,g} = c_{v2v} S^k_{cs} / r_{l,g}$. S^k_{cs} is the size of the intra-platoon consensus log file.

C. Consensus Model

In the intra-platoon consensus, the vehicle with the best V2V communication capabilities or the most abundant resources may be designated as the L_CO. The local consensus within the k-th platoon can be characterized as $A^k_{cs} = \left\{S^k_{cs}, T^k_{\max}\right\}$, where $T^k_{\max}$ is the maximum tolerable intra-platoon consensus delay. Assume that two types of Byzantine faults may occur in the intra-platoon negotiation [10]. One is that the vehicle fails to pass the consensus verification process due to its limited or inaccurate perception, thereby mistakenly voting against the consensus content that should be agreed upon. The other is that the vehicle fails to respond to activate the consensus program despite receiving the consensus file, resulting in the vehicle being judged to vote against the consensus due to a timeout with no feedback. Thus, the PBFT protocol [14], which boasts high Byzantine fault tolerance and is suitable for small-scale scenarios, is employed within the platoon. Suppose $1 - p_{f_1}$ is the probability that a vehicle does not respond, and $1 - p_{f_2}$ is the probability that the perception data is incorrect.

Similarly, in terms of the inter-platoon consensus, the G_CO is chosen from among leader vehicles exhibiting superior 5G-TSN communication capabilities or possessing ample resources. The global inter-platoon consensus can be denoted as $A^{gl}_{cs} = \left\{S^{gl}_{cs}, T^{gl}_{\max}\right\}$, where S^{gl}_{cs} is the size of the inter-platoon consensus log file, and $T^{gl}_{\max}$ is the maximum tolerable inter-platoon consensus delay. Since the main participants in the inter-platoon negotiation are the leader vehicles with a high credibility degree, Byzantine faults occur rarely in the inter-platoon negotiation. In this case, the Raft protocol [13], which possesses a low Byzantine fault tolerance, can be efficiently deployed in such a scenario with low fault tolerance requirements. In addition, the Raft protocol exhibits lower communication complexity and better scalability than the PBFT protocol. Thus, we design a Raft enabled inter-platoon consensus mechanism to meet the time-sensitivity and scalability requirements of multi-platoon negotiation.

Upon receiving a request for multi-platoon negotiation, the G_CO initiates the global multi-platoon consensus. Based on the proposed inter-platoon consensus mechanism, the G_CO packages the consensus content into a log file and multicasts it to all relevant leader vehicles as well as unaffiliated vehicles via 5G-TSN communication. Then, the L_CO organizes the corresponding local consensus verification with the support of V2V communication. The success/failure of the local consensus will be judged by the L_CO following the intra-platoon consensus mechanism. If the local consensus is successful, the leader votes yes in the inter-platoon consensus. Otherwise, it votes no. Meanwhile, unaffiliated vehicles that do not belong to any platoon verify the multi-platoon consensus with their perception. If the verification is successful, they vote yes. Otherwise, they vote no. Let $T^{veri}_{v,un}$ represent the necessary validation delay required for unaffiliated vehicles. Once the intra-platoon consensus or the verification of unaffiliated vehicles is completed, the leader or the unaffiliated vehicle reports its voting result (yes/no) to the G_CO.

At this point, the CUC module gathers the communication requirements and notifies the CNC module after the data is processed. The CNC module determines the configuration and scheduling of each 5G-TSN flow based on the topology of the entire network and the performance of local consensus or the verification of unaffiliated vehicles, such as consensus delay and successful consensus ratio. In accordance with these determinations, the outcomes of the local consensus and unaffiliated vehicle consensus verification are fed back to the G_CO. Subsequently, the G_CO assesses the success of multi-

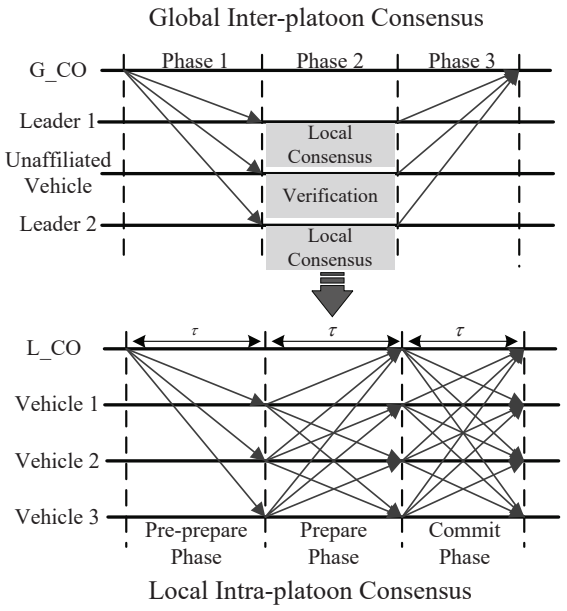

Fig. 2. The operation process of the hierarchical consensus.

platoon consensus according to the inter-platoon consensus mechanism. A successful multi-platoon consensus signifies that the corresponding crucial multi-platoon control decisions are coordinated. The specific hierarchical consensus process is described in Section IV and Section V.

IV. LOCAL CONSENSUS IN A PLATOON

This section proposes a PBFT enabled intra-platoon consensus mechanism with V2V communications and presents a sub-gradient based intra-platoon consensus scheme.

A. PBFT and V2V Based Intra-platoon Consensus Mechanism

Upon receiving a multi-platoon consensus file from the G_CO, the leader will notify the L_CO to organize the local consensus. As depicted at the bottom of Fig. 2, the local consensus comprises three phases: pre-prepare phase, prepare phase, and commit Phase. Following the PBFT protocol [14], during these phases, vehicles need to disseminate identical data to other vehicles within the convoy. Hence, one-to-many communication modes are more aligned with the requirements of the PBFT protocol. With the advancements in V2V sidelink communication facilitated by 5G NR [7], V2V multicast becomes feasible. Thus, we opt for V2V multicast over broadcast to achieve intra-platoon consensus, as it is more bandwidth efficient and enjoys better privacy and security. If the vehicle fails to receive a message within the negotiation interval τ, the transmission is considered unsuccessful. The specific local consensus procedure is delineated below:

Pre-prepare Phase: After receiving the multi-platoon consensus file from the G_CO, the leader vehicle will submit a request to the L_CO to initiate the local consensus verification. Then, the L_CO will enter the pre-prepare phase and send the pre-prepare message to all vehicles in the platoon via V2V multicast communication. Upon receipt of the pre-prepare message and successful response to activate the consensus program, the participant vehicle will transition to the prepare phase. Hence, in the local consensus of the k-th platoon running within the RSU m, the probability that n_k^{pp} vehicles complete the pre-prepare phase and are ready to advance to the next phase can be formulated as

$$Pr_k^{pp}(n_k^{pp}) = \left(p_{f_1} p_{ml}^{pp}\right)^{n_k^{pp}} \left(1 - p_{f_1} p_{ml}^{pp}\right)^{N_k - 1 - n_k^{pp}}, \quad (1)$$

where, p_{ml}^{pp} is the average successful transmission rate of V2V multicast links in the pre-preparation phase.

Moreover, in this phase, the average SINR of the l_k-th V2V multicast link with the g-th channel can be denoted as

$$SINR_{l_k,g}^{pp} = \frac{p^{mul} a_{l_k} h_{l_k}[g]}{\sigma^2 + \sum\limits_{k'=1, k' \neq k}^{K_m} I_{l_k}^{k'}[g]}, \quad (2)$$

where $I_{l_k}^{k'}[g] = \sum\limits_{l_{k'}=1}^{L_{k'}} \delta_{l_{k'}}[g]\, p^{mul} a_{l_{k'}, l_k} h_{l_{k'}, l_k}^{I}[g]$ indicates the interference of the link in the k'-th platoon to the l_k-th link when platoon k and platoon k' are running under the same RSU (interference outside the platoon). $L_{k'}$ is the number of multicast links in the k'-th platoon. p^{mul} is the transmit power of the V2V multicast link, σ^2 is the noise power, and $h[g]$ is the fading gain for the g-th channel. Assume that the fading gain of each channel is independent of each other and follows an exponential distribution with a unit mean. $a_{l_k} = \rho d_{l_k}^{-\alpha}$ denotes the average path loss for the V2V multicast link, ρ is the path loss at the reference distance $d_0 = 1meter$, and α is the path loss index. d_{l_k} is the average distance of the l_k-th V2V multicast link. Vehicles are assumed to be uniformly distributed within the platoon. $a_{l_{k'}, l_k}$ is the average path loss from the transmitter of the $l_{k'}$-th V2V multicast link to the receivers of the l_k-th link. $\delta_l[g]$ is an indicator variable. When $\delta_l[g] = 1$, the g-th channel is assigned to the l-th V2V link.

Therefore, the communication overhead of the k-th platoon in this phase is $O_k^{pp} = \sum\limits_{g=1}^{G} \delta_{l_k}[g]\, o_{l_k,g}^{pp}$.

Prepare Phase: Once in the prepare phase, each participant vehicle (excluding the L_CO) will multicast its own prepare message to all other participants (including the L_CO). When there are no less than $2/3N_k - 1$ prepare messages on a vehicle that come from different participants (including itself) and match the pre-prepare message, the vehicle will verify the reasonableness of the consensus proposal according to its own perception data. If the verification succeeds, the vehicle will conclude the prepare phase and proceed to the commit phase.

For computational purposes, here we assume that the consensus proposal is reasonable, and vehicular verification should be successful unless Byzantine faults arise due to inaccurate vehicular perception. Thus, by utilizing the binomial distribution principle, we can define the probability of a single vehicle concluding the prepare phase and transitioning to the commit phase as

$$p_{v,k}^{pre} = p_{f_2} \sum_{i=\left\lceil \frac{2N_k}{3} - 2 \right\rceil}^{n_k^{pp}-1} \binom{i}{n_k^{pp} - 1} \left(p_{ml}^{pre}\right)^{i} \left(1 - p_{ml}^{pre}\right)^{n_k^{pp} - 1 - i}, \quad (3)$$

where, p_{ml}^{pre} is the average successful transmission rate of the V2V multicast link in the prepare phase. The symbol $\begin{pmatrix} a \\ b \end{pmatrix}$ in equation (3) represents the number of combinations of a samples taken out of b samples at a time with $b \geq a$ and both b and a being non-negative integers. Further, the probability of n_k^{pre} vehicles (including the L_CO) completing the prepare phase and advancing to the commit phase can be expressed as

$$Pr_k^{pre}(n_k^{pre}) = \left(p_{v,k}^{pre}\right)^{n_k^{pre}} \left(1 - p_{v,k}^{pre}\right)^{n_k^{pp}+1-n_k^{pre}}. \quad (4)$$

The average SINR of the l_k-th V2V multicast link with the g-th channel in this phase is

$$SINR_{l_k,g}^{pre} = \frac{p^{mul} a_{l_k} h_{l_k}[g]}{\sigma^2 + I_{in,l_k}^{pre}[g] + \sum\limits_{k'=1,k'\neq k}^{K_m} I_{l_k}^{k'}[g]}, \quad (5)$$

where, $I_{in,l_k}^{pre}[g] = \sum\limits_{l=1,l\neq l_k}^{L_k-1} \delta_l[g]\, p^{mul} a_{l,l_k} h_{l,l_k}^I[g]$ represents the interference caused by the multicast link within the k-th platoon (interference inside the platoon). The communication overhead in this phase is $O_k^{pre} = \sum\limits_{l_k=1}^{L_k-1} \sum\limits_{g=1}^{G} \delta_{l_k}[g]\, o_{l_k,g}^{pre}$.

Commit Phase: In this phase, vehicles (including the L_CO) will multicast their own commit messages to other vehicles. When a vehicle collects no fewer than $2/3N_k$ commit messages from different participants (including itself), the local consensus is considered successful [14]. Subsequently, the leader vehicle of the platoon will report the local consensus result to the G_CO via 5G-TSN communications.

Let p_{ml}^{com} be the successful transmission rate of the multicast link in this phase. The probability that the vehicle receives a commit message from n_k^{com} distinct participants (excluding itself) can be calculated as

$$Pr_k^{com}(n_k^{com}) = \left(p_{ml}^{com}\right)^{n_k^{com}} \left(1 - p_{ml}^{com}\right)^{n_k^{pre}-1-n_k^{com}}. \quad (6)$$

The average SINR of the l_k-th V2V multicast link with the g-th channel in this phase is

$$SINR_{l_k,g}^{com} = \frac{p^{mul} a_{l_k} h_{l_k}[g]}{\sigma^2 + I_{in,l_k}^{com}[g] + \sum\limits_{k'=1,k'\neq k}^{K_m} I_{l_k}^{k'}[g]}, \quad (7)$$

with $I_{in,l_k}^{com} = \sum\limits_{l=1,l\neq l_k}^{L_k} \delta_l[g]\, p^{mul} a_{l,l_k} h_{l,l_k}^I[g]$. The SINR in equations (2), (5), and (7) will be used to calculate the lower bounds of p_{ml}^{pp}, p_{ml}^{pre} and p_{ml}^{com}. The specific calculation process is described in Section IV-B2. The communication overhead in this phase is $O_k^{com} = \sum\limits_{l_k=1}^{L_k} \sum\limits_{g=1}^{G} \delta_{l_k}[g]\, o_{l_k,g}^{com}$.

B. Performance Analysis

1) Local consensus delay analysis: As illustrated in Fig. 2, the negotiation process in the intra-platoon consensus is split into multiple slots with fixed intervals τ. The delay of the whole local consensus process in the k-th platoon can be defined as $T_{cs}^k = 3 * \tau$.

2) Analysis of the successful intra-platoon consensus ratio: Assume that $SINR_{\min}^k$ is the minimum SINR required by the receiver to successfully receive the message within a negotiation interval. With given τ, the $SINR_{\min}^k$ can be written as $2^{GS_{cs}^k/B\tau} - 1$. Based on the $SINR_{\min}^k$ and the SINR of each consensus phase, the lower bound of p_{ml}^{pp}, p_{ml}^{pre} and p_{ml}^{com} can be obtained. The calculation process is described in Appendix A. In this way, the probabilistic analysis model of the successful local consensus ratio P_{cs}^k can be accurately represented by equation (8).

C. An Adaptive Intra-platoon Consensus Scheme

Inappropriate local consensus negotiation interval τ and channel allocation of V2V communication may lead to an excessive delay or a low successful consensus ratio in the intra-platoon consensus, subsequently impacting the global consensus. Therefore, it is imperative to formulate an optimization problem to minimize the local consensus delay while improving the successful intra-platoon consensus ratio. The optimization problem is formulated as

$$\begin{aligned} \min_{\delta_{l_k}[g],\tau_k} \quad & T_{cs}^k \\ s.t. C1 \quad & \delta_{l_k}[g] \in \{0,1\}, l_k \in L_k, g \in G \\ C2 \quad & T_{cs}^k \leq T_{\max}^k \\ C3 \quad & P_{cs}^k \geq P_{cs,k}^{\min} \\ C4 \quad & \sum_{g=1}^{G} \delta_{l_k}[g] = 1, l_k \in L_k \\ C5 \quad & O_k^{pp} + O_k^{pre} + O_k^{com} \leq C_{cs}^k \end{aligned} . \quad (9)$$

$P_{cs,k}^{\min}$ is the minimum tolerable successful local consensus ratio in the k-th platoon. C_{cs}^k is the maximum expected communication cost for local consensus requests in the k-th platoon. Constraint C1 gives the domain of $\delta_{l_k}[g]$. Constraint C2 indicates that the local consensus needs to be accomplished within the maximum tolerable intra-platoon delay constraint. Constraint C3 demonstrates that the current successful local consensus ratio must be greater than $P_{cs,k}^{\min}$. Constraint C4 illustrates that each V2V multicast link can only choose one channel to transmit. Constraint C5 denotes the local communication cost constraint.

Since equation (9) is a non-convex problem, the sub-gradient descent algorithm combined with the Lagrangian multiplier method can be utilized to acquire the optimal strategy. The Lagrangian relaxation function of the target problem can be expressed as $L(\delta_{l_k}, \tau_k, \mathbb{U})$ with multipliers set $\mathbb{U}$. The Lagrangian dual problem of the original problem can be shown as $\max\limits_{\mathbb{U}} g(\mathbb{U}) = \max\limits_{\mathbb{U}} \inf\limits_{\{\delta_{l_k},\tau_k\}} L(\delta_{l_k}, \tau_k, \mathbb{U})$. By differentiating $L(\delta_{l_K}, \tau_k, \mathbb{U})$ with respect to δ_{l_k}, τ_k and letting them equal to zero, we can get a feasible solution $\{\delta_{l_k}, \tau_k\}$ of the internal minimization problem for the given multipliers $\mathbb{U}$. As the differentiability of $g(\mathbb{U})$ cannot be ensured, the traditional gradient descent method is unsuitable for addressing the external maximization problem. The sub-gradient algorithm [29], as an extension of the traditional gradient descent algorithm, provides an effective approach for solving optimization problems with non-differentiable functions. Thus, in our proposed

$$P_{cs}^{k}(p_{ml}^{pp}, p_{ml}^{pre}, p_{ml}^{com}) = \sum_{n_k^{pp}=\lceil \frac{2N}{3}-1 \rceil}^{N-1} \begin{pmatrix} n_k^{pp} \\ N-1 \end{pmatrix} Pr_k^{pp}(n_k^{pp}) * \sum_{n_k^{pre}=\lceil \frac{2N}{3} \rceil}^{n_k^{pp}+1} \begin{pmatrix} n_k^{pre} \\ n_k^{pp}+1 \end{pmatrix} Pr_k^{pre}(n_k^{pre}) * \sum_{n_k^{com}=\lceil \frac{2N}{3}-1 \rceil}^{n^{pre}-1} \begin{pmatrix} n_k^{com} \\ n_k^{pre}-1 \end{pmatrix} Pr_k^{com}(n_k^{com}) \quad (8)$$

Algorithm 1 The Adaptive Intra-platoon Consensus Scheme

1: Initializes the Lagrangian multiplier sets $\mathbb{U}(t)$
2: **for** The number of iterations $t \in [0, 1, 2, ..., t_{\max}]$ **do**
3: With the given multiplier sets $\mathbb{U}(t)$, differentiate $L\left(\delta_{l_K}, \tau_k, \mathbb{U}\right)$ with respect to δ_{l_k}, τ_k and let them equal to zero to get a feasible solution $\left\{\delta_{l_k}, \tau_k\right\}$ of $\inf_{\{\delta_{l_k}, \tau_k\}} L\left(\delta_{l_k}, \tau_k, \mathbb{U}\right)$.
4: Update the multiplier set $\mathbb{U}(t+1)$ with sub-gradient algorithm.
5: **if** $\mathbb{U}(t+1) - \mathbb{U}(t) \leq \varepsilon$ **then**
6: Return the feasible solution;
7: Break;
8: **else**
9: Continue;
10: **end if**
11: **end for**

scheme, $\mathbb{U}$ will be updated by the sub-gradient algorithm based on the feasible solution $\left\{\delta_{l_k}, \tau_k\right\}$ to find a solution to the external maximization problem. The optimal solution of the objective function can be obtained by repeating the above steps until the multipliers converge to a preset threshold. The main steps of the proposed adaptive intra-platoon consensus scheme with jointly designing the consensus slot length and channel allocation are delineated in Algorithm 1.

V. The inter-platoon consensus

In this section, we investigate the inter-platoon consensus mechanism. We apply the Raft protocol to improve the time-sensitivity and scalability of multi-platoon negotiations. In addition, we develop an optimal 5G-TSN flow scheduling algorithm to support the inter-platoon consensus. DDPG is employed to derive the optimal strategy, ensuring the successful multi-platoon consensus while reducing the total delay.

A. Raft enabled Inter-platoon Consensus Mechanism

The consensus process is illustrated at the top of Fig. 2. It has three main phases:

Phase 1: Once receiving a request for a multi-platoon consensus, the G_CO will package the proposal content into a log file and identify the platoons and unaffiliated vehicles participating in the consensus. Assume that the G_CO can obtain the trajectories, communication capabilities, and geographic distance from the event location of platoons and unrelated vehicles in the current area from the centralized control unit. Based on this information, the G_CO will determine which platoons/unaffiliated vehicles are best positioned and equipped to participate in the consensus process effectively. This ensures that only those platoons/unaffiliated vehicles that can provide valuable input and have a direct stake in the consensus outcome are included. Then, leveraging 5G-TSN technology, the G_CO will send log files to all participants via multicast.

Phase 2: Then, depending on a successful receipt of the global consensus file, leader vehicles will request to initiate the local consensus verification within the platoon. The intra-platoon consensus will adopt the proposed PBFT and V2V enabled consensus mechanism, which is depicted in Section IV-A. Unaffiliated vehicles will commence the validation of global consensus content with their own perceptions.

Phase 3: When the local consensus is completed, leader vehicles will return the results to the G_CO via 5G-TSN communication. And unaffiliated vehicles will report their feedback once their verification is completed.

According to the Raft protocol, a successful multi-platoon consensus relies on more than half of the intra-platoon vehicles and unaffiliated vehicles voting yes and relaying their results to the G_CO within the delay constraint [13]. After evaluating the results of the global consensus according to the Raft protocol, once the consensus is successful, the G_CO will notify all relevant platoons and vehicles to execute the decision via the 5G-TSN broadcast communication. Otherwise, the G_CO will reorganize the consensus, or the centralized control unit in the edge cloud will remake the critical multi-platoon control decision.

B. Delay Analysis

The total delay of the k-th platoon receiving a multi-platoon consensus file, accomplishing the local consensus validation, and successfully feeding back to the G_CO can be derived as

$$T_{tol}^{k} = T^{ph1} + T_{cs}^{k} + T_{f_k}, \quad (10)$$

where, T^{ph1} is the transmission delay of the multicast of the multi-platoon consensus file in Phase 1 and T_{f_k} is the transmission delay of the 5G-TSN flow f_k between the leader vehicle of the k-th platoon and the G_CO in Phase 3.

Similarly, the total delay for the v-th unaffiliated vehicle to finish the multi-platoon consensus is $T_{tol}^{v} = T^{ph1} + T_{v,un}^{veri} + T_{f_v}$. T_{f_v} is the transmission delay of the 5G-TSN flow f_v between the unaffiliated vehicles and the G_CO in Phase 3.

Let r_{f_k} and r_{f_v} be the routing paths of flow f_k and flow f_v, respectively. $\left|r_{f_k}\right|$ and $\left|r_{f_v}\right|$ are the number of TSN GWs that flow f_k and f_v pass, respectively. The end-to-end delay of flow f_k in the 5G-TSN network is

$$T_{f_k} = t_{f_k}^{5G} + \left|r_{f_k}\right| t^{pc} + (\left|r_{f_k}\right| - 1)(t^{pg} + t_{f_k}^{tr}) + \sum_{i=1}^{r_{f_k}} t_{i,f_k}^{qu}, \quad (11)$$

where, $t_{f_k}^{5G} = S_{cs}^{gl}/\gamma_{So_{f_k}}^{5G} + S_{cs}^{gl}/\gamma_{De_{f_k}}^{5G}$ represents the transmission delay of flow f_k in 5G RAN. The same goes for T_{f_v}.

$\gamma_{So_{f_k}}^{5G}$ and $\gamma_{De_{f_k}}^{5G}$ are the transmission rates of the 5G RAN where the source vehicle and destination vehicle of flow f_k are located, respectively. t^{pc} and $t_{f_k}^{tr} = S_{cs}^{gl}/\gamma_{tsn}$ are the processing delay and transmission delay of the TSN GW, respectively. γ_{tsn} is the transmission rate of the TSN network. t^{pg} is the propagation delay of a single link in the TSN network. And t_{i,f_k}^{qu} is the queuing delay of the f_k on the i-th TSN GW. Suppose that t^{pc} is the same for all GWs and t^{pg} is the same for all links. Each TSN GW will divide flows into different queues based on their priority. Flows with higher priority will be forwarded first. While flows within the same queue will follow the first-come-first-served principle.

C. A Dynamic Prioritization Scheme for 5G-TSN Flows

The delay and success rate of intra-platoon consensus exerts a significant impact on the global consensus performance. Considering the discrepancies in local consensus results delivered through each 5G-TSN flow, the prioritization of 5G-TSN flows should be dynamically configured according to the corresponding local consensus performance. This dynamic prioritization adjustment is important in ensuring the real-time and successful consensus of multi-platoon negotiations. Therefore, we devise an integrated adaptive priority configuration scheme aimed at delivering data within the constraints of multi-platoon consensus.

The priority of the flow f_k between the leader vehicle of the k-th platoon and the G_CO in Phase 3 is

$$\omega_{f_k} = \left\lfloor \Omega \left(\frac{1 - P_{cs}^{k}}{1 - P_{v/k}^{\min}} \right) \left(\frac{T_{\max}^{gl} - T_{cs}^{k}}{T_{\max}^{gl} - T_{\min}^{v/k}} \right) \right\rfloor, \tag{12}$$

where, Ω is the total number of priority levels, $T_{\min}^{v/k} = \min(T_{cs}^{k}, T_{v,un}^{veri})$ and $P_{v/k}^{\min} = \min(P_{cs}^{k}, P_{v,un}^{veri})$.

It is noted that ω_{f_k} will diminish as the successful local consensus ratio increases and the remaining time decreases. The smaller the ω_{f_k}, the higher the priority it represents. Local consensus with higher success rates plays a more important role in promoting the success of global consensus. $\lfloor * \rfloor$ is an integer value obtained by rounding down. Similarly, the priority of the flow f_v is $\omega_{f_v} = \left\lfloor \Omega \left(\frac{1-P_{v,un}^{veri}}{1-P_{v/k}^{\min}} \right) \left(\frac{T_{\max}^{gl} - T_{v,un}^{veri}}{T_{\max}^{gl} - T_{\min}^{v/k}} \right) \right\rfloor$. $P_{v,un}^{veri}$ is the probability that the unaffiliated vehicle votes yes.

In this way, our proposed priority configuration scheme can offer foundational guidance for the design of 5G-TSN flow routing in Section V-D. This aids the network system in allocating resources and optimizing path selection more efficiently. As a result, as much consensus feedback as possible can be delivered to the G_CO to facilitate the success of the global consensus.

D. A DDPG Based Inter-platoon Consensus Scheme

As elaborated in Section V-B, distinct 5G-TSN flow routing strategies correspond to different end-to-end latency. According to the technical principle of 5G-TSN, only one frame can be transmitted on a single TSN link at any given time. In other words, the transmission windows of frames on the same egress port of a TSN GW cannot overlap [30]. Consequently, an inappropriate flow scheduling strategy may result in an excessive queuing delay, subsequently impacting the total delay of multi-platoon negotiations. To enhance the responsiveness of multi-platoon negotiations, it becomes essential to devise a suitable 5G-TSN flow scheduling scheme based on the priority configuration in Section V-C. The detailed optimization problem can be formulated as equation (13). By solving this problem, the optimal scheduling strategy with the minimum global consensus delay can be obtained, and the success of the multi-platoon consensus can be ensured to improve the coordination of multi-platoon cooperative control.

$$\begin{aligned}
&\min_{r_{f_k}, r_{f_v}} \quad \frac{\sum_{m=1}^{M} \left(\sum_{k=1}^{K_m} T_{tol}^{k} + \sum_{v=1}^{V_m} T_{tol}^{v} \right)}{\sum_{m=1}^{M} (K_m + V_m)} \\
&s.t. C1 \ \sum_{m=1}^{M} \{ \sum_{k=1}^{K_m} x_{a,b}^{f_k}(t) + \sum_{v=1}^{V_m} x_{a,b}^{f_v}(t) \} \le 1, a \in M, b \in M \ . \\
&C2 \ \frac{\sum_{m=1}^{M} \{ \sum_{k=1}^{K_m} if\left(T_{tol}^{k} \le T_{\max}^{gl}\right) P_{cs}^{k} N_k + \sum_{v=1}^{V_m} if\left(T_{tol}^{v} \le T_{\max}^{gl}\right) P_{v,un}^{veri} \}}{\sum_{m=1}^{M} \left(\sum_{k=1}^{K_m} N_k + V_m \right)} > 50\%
\end{aligned} \tag{13}$$

$x_{a,b}^{f_k}(t)$ is an indicator variable. $x_{a,b}^{f_k}(t) = 1$ represents that the flow f_k is transmitted on the link between TSN GW a and TSN GW b at time slot t. The same goes for $x_{a,b}^{f_v}(t)$. Constraint C1 indicates that, in order to achieve the deterministic transmission of 5G-TSN flows, at most one frame can be transmitted on a link at any time [30]. Suppose that the log file of global consensus can be sent within one frame. When $T_{tol}^{k} \le T_{\max}^{gl}$, $if\left(T_{tol}^{k} \le T_{\max}^{gl}\right) = 1$. The same principle applies to $if\left(T_{tol}^{v} \le T_{\max}^{gl}\right)$. Constraint C2 guarantees the achievement of the successful global consensus, which is defined as more than half of the platoons and unaffiliated vehicles successfully reaching local consensus or validation and reporting the feedback to G_CO within the maximum tolerable global consensus delay constraint.

In equation (13), due to constraint C1, the scheduling of 5G-TSN flows of one leader vehicle will not only affect its own delay in completing the consensus, but also affect the delay of other leader vehicles and unaffiliated vehicles. Hence, the optimal strategies form a complex set with tight coupling relations. It is hard to calculate the optimal solution directly. To address this problem, we formulate equation (13) as a Markov Decision Process (MDP) and design a DDPG based optimal scheduling scheme for global inter-platoon consensus. $\langle S, A, P, \varphi \rangle$ represents the MDP framework, where S is the state space, A is the action space, P is the state transition probability, and φ is the instant reward with action A and state S. Assume that $path_{r,f_i}$ is the set of all available paths for flow f_i. p_{r,f_i} is the set of the chosen probabilities for each path in the $path_{r,f_i}$ set.

The state space at time t can be described as

$$S^t = \left\{ p_{r,f_k}^t, p_{r,f_v}^t \right\}, k \in K_m, v \in V_m, m \in M. \tag{14}$$

The action space can be expressed as

$$A^t = \left\{ \Delta p_{r,f_{k_1}}^t, ..., \Delta p_{r,f_{K_M}}^t, \Delta p_{r,f_{v_1}}^t, ..., \Delta p_{r,f_{V_M}}^t \right\}, \tag{15}$$

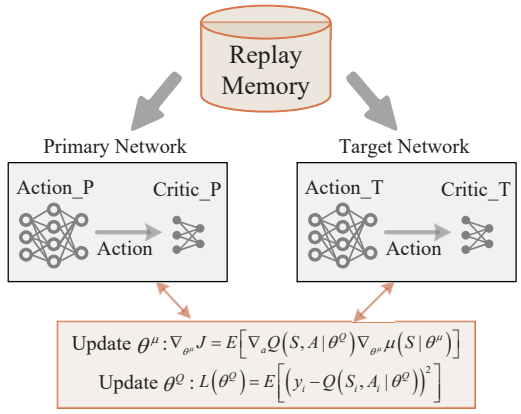

Fig. 3. Architecture of DDPG based scheme.

where Δx is the adjustment to x. With A^t and S^t, r_{f_i} can be selected from $path_{r,f_i}$ based on the probability set p_{r,f_i}. Thus, the instant system utility is

$$\varphi^t = T_{\max}^{gl} - \frac{\sum_{m=1}^{M}\left(\sum_{k=1}^{K_m} T_{tol}^k + \sum_{v=1}^{V_m} T_{tol}^v\right)}{\sum_{m=1}^{M}(K_m + V_m)}. \tag{16}$$

To maximize the utility of multi-platoon consensus, the optimal scheduling strategy for 5G-TSN flows π^* needs to be obtained. Here, π^* can be shown as $\pi^* = \arg\max_{\pi} E\left(\sum_{t=1}^{\infty} \eta^t \varphi^t\right)$. π represents a strategy set and η is a discounting factor that trades off the immediate utility and the later ones.

By combining the actor-critic approach with the learning process of deep Q-network, DDPG becomes a potentially feasible solution for deriving the optimal scheduling strategy π^* for global inter-platoon consensus. A DDPG agent learns directly from the unprocessed observation space through the policy gradient algorithm for estimating the weight of the policy. Meanwhile, the actor-critic model is employed to learn the value function and update the actor model. Since DDPG leverages the stochastic behavior policy for strategy exploration, effectively reducing the complexity of the learning process, it is ideally suited to address the challenges presented by high-dimensional and continuous action spaces. Given that the action space in the proposed MDP consists of high-dimensional variables, DDPG emerges as a preferred algorithm to address the above problems.

Fig. 3 shows the architecture of DDPG, which mainly consists of the primary network and the target network. Each network has an actor and a critic. The actor and the critic are two different deep neural networks. Based on the current observation space, the actor of the primary network will explore the scheduling strategy and get the corresponding system utility φ^t. Then, the agent will update the critic network of the primary network according to the φ^t and update the actor network of the primary network in the direction suggested by its critic. The target network can be taken as an old version of the primary one, which generates the target value for training the primary network. The learning experience of action, reward, and state transition will be stored in the replay memory, and be used to train the parameters of actor and critic networks. The main steps of the proposed DDPG based flow scheduling scheme for inter-platoon consensus are summarized as Algorithm 2.

Algorithm 2 A DDPG Based Optimal Flow Scheduling Scheme for Inter-platoon Consensus

1: Initialize critic function $Q(S, A|\theta^{\mu})$ and actor function $\mu(S|\theta^Q)$ with randomly chosen parameters θ^Q and θ^{μ},respectively; Initialize target critic function Q' and target actor function μ' with $\theta^{Q'} = \theta^Q$ and $\theta^{\mu'} = \theta^{\mu}$; Initialize experience replay buffer.
2: **for** each episode **do**
3: Initialize the environment information;
4: Acquire the results of each local consensus through Algorithm 1; Calculate the priority of each 5G-TSN flow as described in Section V-C; Then, derive the initial state set;
5: **for** t = 1 to max-episode-length **do**
6: Get the action set A^t according to the actor-critic model under the constraints of equation (13);
7: Execute the action, calculate the reward φ^t and new state set S^{t+1} according to equation (16);
8: Store the experience $(S^t, A^t, \varphi^t, S^{t+1})$ into the experience replay buffer;
9: Get a batch of samples $(S^i, A^i, \varphi^i, S^{i+1})$ from the replay memory, let $y_i = \varphi^i + \eta Q'\left(S^{i+1}, \mu'\left(S^{i+1}|\theta^{\mu'}\right)|\theta^{Q'}\right)$;
10: Update θ^Q by minimizing the loss function: $L\left(\theta^Q\right) = E\left[\left(y_i - Q\left(S_i, A_i|\theta^Q\right)\right)^2\right]$.
11: Update θ^{μ} by using the policy gradient: $\nabla_{\theta^{\mu}} J = E\left[\nabla_a Q\left(S, A|\theta^Q\right) \nabla_{\theta^{\mu}} \mu\left(S|\theta^{\mu}\right)\right]$.
12: Update target networks with $\theta^{Q'} = \varpi\theta^Q + (1-\varpi)\theta^{Q'}$ and $\theta^{\mu'} = \varpi\theta^{\mu} + (1-\varpi)\theta^{\mu'}$, where $0 < \varpi \ll 1$.
13: **end for**
14: **end for**

VI. Performance Evaluation

We evaluate the performance of our proposed HCVN scheme for multi-platoon cooperative control. In our experiments, we set $M = 5$ and the number of platoons K_m within an RSU is randomly chosen from (1, 4) units. The number of vehicles N_k in a platoon (i.e., platoon size) is randomly set from (5, 25) units and the number of unaffiliated vehicles V_m in an RSU is randomly chosen from (5, 15) units. Following the settings in [24] and [1], the other parameters are selected randomly from the intervals in Table I.

Fig. 4 illustrates the convergence of our proposed sub-gradient based adaptive intra-platoon consensus scheme implemented in different scenarios. These scenarios have different platoon numbers, unaffiliated vehicle numbers, and platoon sizes. The detailed parameters are listed in Table II. In different scenarios, the algorithm converges at around 150 iterations.

Fig. 5 shows the convergence of the proposed DDPG-based inter-platoon consensus scheme in different scenarios,

TABLE I
PARAMETERS VALUES

Parameter	Value
Maximum tolerable intra-platoon consensus delay $T^k_{\max}$	(3, 10) ms
Intra-platoon consensus file size S^k_{cs}	(6000, 8000) Bytes
Maximum tolerable inter-platoon consensus delay $T^{gl}_{\max}$	(10, 14) ms
Inter-platoon consensus file size S^{gl}_{cs}	(15000, 30000) Bytes
Minimum tolerable local successful consensus ratio $P^{\min}_{cs,k}$	(75, 95)%
Probability of unaffiliated vehicle voting yes $P^{veri}_{v,un}$	(30, 75)%
Probability of vehicle non-response $1 - p_{f_1}$	(1, 5)%
Probability of incorrect vehicular perception $1 - p_{f_2}$	(1, 5)%
V2V communications Bandwidth B	100 MHz
Number of V2V communication channels G	8 channels
Transmit power of V2V multicast links p^{mul}	23 dBm
Noise power σ^2	-114 dBm
Path loss index α	3
Path loss at 1 meter ρ	- 20 dB
RSU coverage d_{RSU}	100 meters
Minimum vehicle spacing $d^{\min}_v$	3.5 meters
Total number of priorities for TSN flows Ω	3
Transmission rate of TSN network γ_{tsn}	1 Gbit/s
Processing delay of TSN GW t^{pc}	1.5 μs

TABLE II
PARAMETERS VALUES IN DIFFERENT SCENARIOS

	Scenario 1	Scenario 2	Scenario 3	Scenario 4
Platoon Number	8 units	16 units	12 units	10 units
Platoon Size	8 units	8 units	6 units	10 units
Unaffiliated Vehicles Number	10 units	5 units	15 units	30 units

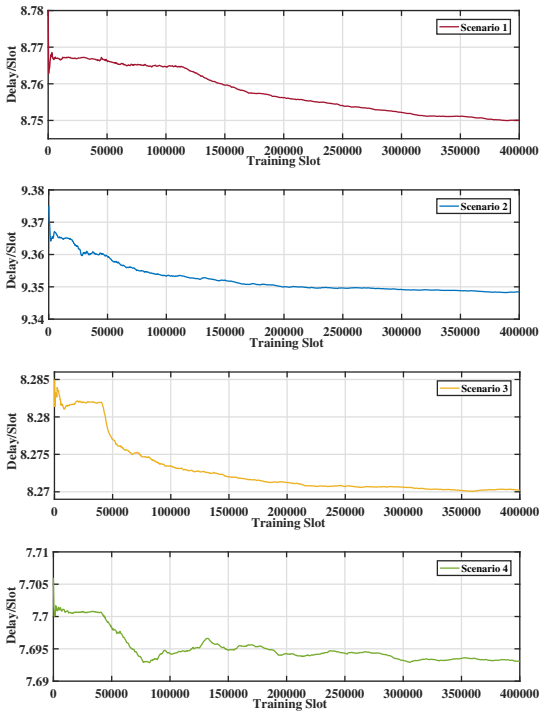

Fig. 5. Convergence of our proposed DDPG based inter-platoon consensus scheme.

respectively. Despite the difference in the application scale of the scenarios, all the delay consumed by our scheme achieves convergence after about 300,000 training slots.

Fig. 6 exhibits the comparison of coordination degree and total negotiation delay of multi-platoon cooperative control in various scenarios with different schemes. In the scheme without negotiation, platoons and unaffiliated vehicles make critical control decisions based on their perception and execute them directly. ${p_a}^N$ represents the overall coordination among multiple vehicles in the non-negotiation scheme with N vehicles and p_a perceptual accuracy. Suppose p_a is 98%. In the schemes with negotiation, the overall coordination is indicated by the successful consensus ratio, which is described in Section III-C.

As depicted in Fig. 6, compared with the scheme without vehicular negotiation, those incorporating negotiation exhibit higher coordination degrees. In addition, solutions with 5G-TSN support and based on Hierarchical Consensus (HC) demonstrate significantly higher coordination degrees than the single-layer PBFT based solution without 5G-TSN support. This discrepancy arises because the single-layer PBFT based scheme without 5G-TSN support can only realize vehicular negotiation within the platoon. In contrast, with the help of 5G-TSN, HC based solutions not only achieve the intra-platoon consensus but also enable fast negotiation among platoons as well as between platoons and unaffiliated vehicles. This results in a substantial improvement of the coordination indicator from 0.1 - 0.45 to 0.58 - 0.82, accompanied by a slight increase of about 1 - 2.5 ms in total negotiation delay. Among the three HC based approaches, greedy routing (tends to choose the shortest path) and random routing methods may induce excessive queuing delays for 5G-TSN flows. This exacerbates the challenge of implementing multi-platoon negotiation within delay constraints and leads to large negotiation delays. Unlike these two schemes, our proposed HCVN scheme leverages HC to enhance the vehicular coordination, while dynamically adjusting the intra-platoon channel allocation and inter-platoon 5G-TSN flow scheduling strategies through the sub-gradient based intra-platoon consensus algorithm and the DDPG based inter-platoon consensus approach. Obviously, our proposed approach attains the highest coordination and the lowest total negotiation delay.

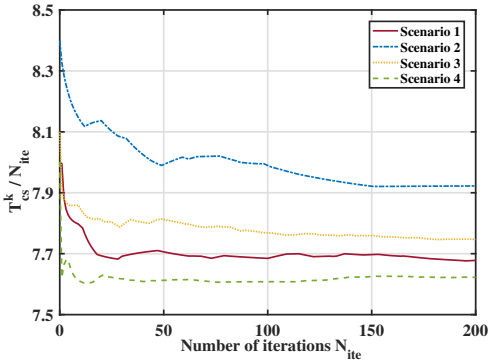

Fig. 4. Convergence of the proposed adaptive intra-platoon consensus scheme.

Fig. 7 presents the intra-platoon consensus delay T^k_{cs} with different platoon sizes, vehicle non-response probabilities $1 - p_{f_1}$, and perception error probabilities $1 - p_{f_2}$ under fixed bandwidth. Since the platoon size has too much influence on the T^k_{cs}, in order to facilitate the display in the same axis, we use the difference between T^k_{cs} (with various p_{f_1}, p_{f_2}) and the standard value T^*_{cs} (with $p_{f_1} = 0.99$, $p_{f_2} = 0.99$)

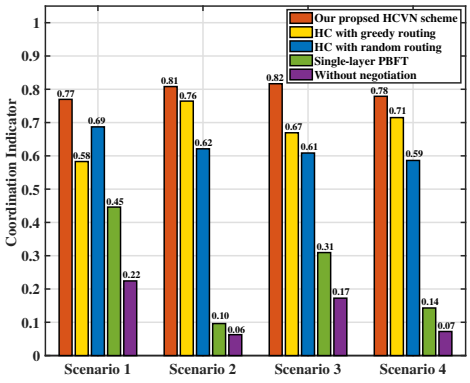

(a) Comparison of coordination indicator.

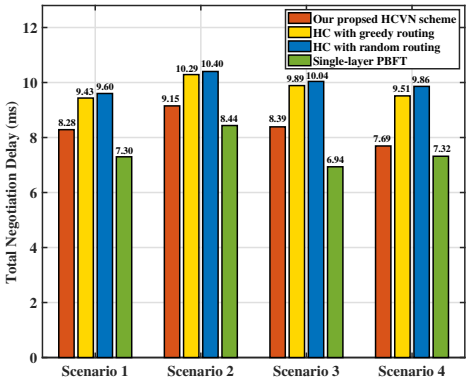

(b) Comparison of total negotiation delay.

Fig. 6. Coordination indicator and total negotiation delay of multi-platoon cooperative control in each scenario with different schemes.

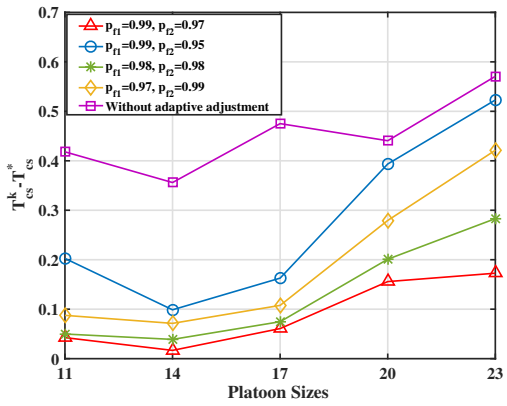

Fig. 7. The difference between intra-platoon consensus delay T^k_{cs} (with various p_{f_1}, p_{f_2}) and T^*_{cs} (with $p_{f_1} = 0.99$, $p_{f_2} = 0.99$).

as the ordinate. This figure indicates that the T^k_{cs} of our proposed adaptive local consensus scheme is lower than the scheme without adaptive adjustment. As p_{f_1} and p_{f_2} decrease, T^k_{cs} becomes larger. Since, when the number of incorrect vehicles increases, the platoon leader tends to extend the local consensus time to obtain more verification information from other correct vehicles. Nevertheless, the delay of the green line is lower than that of the yellow line because the effect of p_{f_2} on T^k_{cs} is less than the effect of p_{f_1} on T^k_{cs}. Specifically, the reduction in p_{f_2} affects the probability of a vehicle voting yes on the consensus content, having a limited effect on

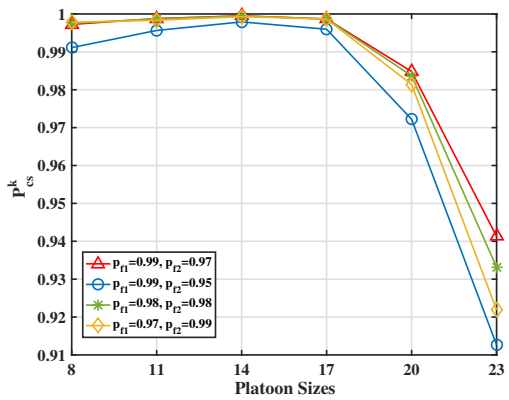

Fig. 8. Successful intra-platoon consensus ratio with various p_{f_1}, p_{f_2}, platoon sizes and fixed bandwidth.

T^k_{cs}. In contrast, the decreased p_{f_1} hinders the vehicle from responding to consensus requests, which will significantly lengthen the time required to complete the consensus. Besides, the impact of changes in p_{f_1} and p_{f_2} on $T^k_{cs} - T^*_{cs}$ becomes smaller and then greater as the platoon size increases. This is because when p_{f_1} and p_{f_2} are less than the standard value $p_{f_1} = 0.99$, $p_{f_2} = 0.99$, the increase in the number of vehicles within a platoon can compensate for the lack of p_{f_1} and p_{f_2}, making the $T^k_{cs} - T^*_{cs}$ smaller. However, due to the limited communication bandwidth, too many vehicles will reduce the transmission rate of V2V communication and make the disadvantages of smaller p_{f_1} and p_{f_2} more obvious, resulting in a gradually larger $T^k_{cs} - T^*_{cs}$.

Fig. 8 exhibits the effect of different p_{f_1}, p_{f_2} on successful intra-platoon consensus ratio with different platoon sizes. To facilitate the observation of changes, we set the intra-platoon consensus delay at 7.5 ms. When the number of vehicles participating in the intra-platoon consensus increases, the influence of p_{f_1}, p_{f_2} on the consensus gradually decreases, and the P^k_{cs} becomes larger first. Then, with the fixed communication bandwidth and consensus delay, too many participating vehicles will enhance the communication interference within the platoon and reduce the successful transmission rate of V2V communication, leading to the subsequent decrease of P^k_{cs}. Moreover, the lower p_{f_1} and p_{f_2} are, the lower the P^k_{cs} will be. It is noteworthy that the P^k_{cs} of the red line is higher than that of the yellow line, which means that the reduction of p_{f_1} has a more severe impact on P^k_{cs} than the reduction of p_{f_2}.

Fig. 9 demonstrates the impact of varying platoon numbers and unaffiliated vehicle numbers on total negotiation delay. With an identical number of unaffiliated vehicles, increasing the count of platoons decreases the communication transmission rate within the platoon, resulting in a growth in the time required for the leader vehicle to complete the local consensus. When the number of platoons reaches 10 to 14, the local consensus delay approaches $T^k_{\max}$, causing a plateau increase in the total negotiation delay. Nevertheless, once the number of platoons exceeds 14, the total delay rises rapidly again because of the increase in 5G-TSN flows and the growth of queuing delay in the TSN network. Furthermore, due to the comparatively lower reliability and coordination of unaffiliated

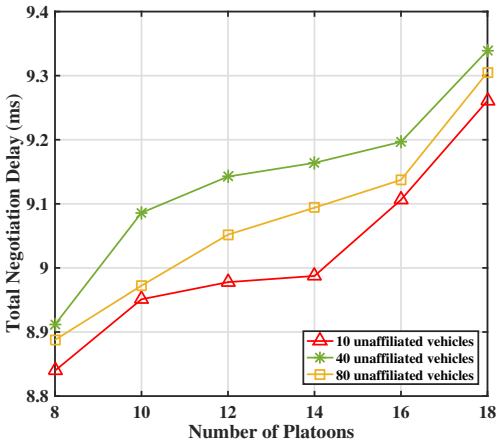

Fig. 9. Total negotiation delay with various platoon numbers, unaffiliated vehicles and fixed bandwidth.

vehicles compared to intra-platoon vehicles, an increase in the number of unaffiliated vehicles results in a delay in achieving successful multi-platoon consensus. However, the total delay with 80 unaffiliated vehicles is lower than the total delay with 40 unaffiliated vehicles, which indicates that even if the unaffiliated vehicles are poorly reliable, a large number of unaffiliated vehicles still contributes to the success of multi-platoon consensus.

VII. Conclusion

In this article, we proposed a new hierarchical consensus framework for efficient multi-platoon negotiation in cooperative platooning. For intra-platoon consensus, we utilized the PBFT protocol and designed an adaptive scheme to reduce local consensus delay and improve the successful local consensus ratio. For inter-platoon consensus, we proposed a new Raft and 5G-TSN enabled scheme, supported by a DDPG-based flow scheduling algorithm to minimize the total negotiation delay while ensuring the success of multi-platoon negotiations. Simulation results showed that our proposed schemes can reduce the local consensus delay by 9.2%, decrease the total negotiation delay by more than 14%, and enhance the coordination indicator of multi-platoon cooperative control by more than 16.9% compared to the existing solutions. It is obvious that our proposed HCVN scheme can quickly and reliably achieve tight coordination within platoons as well as among platoons with unaffiliated vehicles.

Appendix A
Calculation of p_{ml}^{pp}, p_{ml}^{pre} and p_{ml}^{com}

With $SINR_{\min}^{k}$, the average successful transmission rate of V2V multicast links in pre-prepare phase p_{ml}^{pp} can be expressed as

$$\begin{aligned} p_{ml}^{pp} &= 1 - pr\left(\overline{SINR_k^{pp}} \le SINR_{\min}^{k}\right) \\ &= 1 - E\left\{u\left(SINR_{\min}^{k} - \overline{SINR_k^{pp}}\right)\right\}, \end{aligned} \tag{17}$$

where $u(\cdot)$ is the step function [31]. To simplify the calculation, the step function can be replaced by its smoothing approximation function $u_\theta(x) = \left(1+e^{-\theta x}\right)^{-1}$. θ is a non-negative smooth parameter which is related to the approximation error [32]. Since $u_\theta(x)$ is a concave function, the lower bound of p_{ml}^{pp} can be obtained as

$$\begin{aligned} p_{ml}^{pp} &\cong 1 - E\left\{u_\theta\left(SINR_{\min}^{k} - \overline{SINR_k^{pp}}\right)\right\} \\ &\ge 1 - u_\theta\left(SINR_{\min}^{k} - \overline{E\left\{SINR_{l_k,g}^{pp}\right\}}\right) \end{aligned}, \tag{18}$$

by using Jensen's inequality.

Vehicles are assumed to be uniformly distributed within the platoon. Platoons are uniformly distributed within the coverage area of RSU. The expect function $E\left\{SINR_{l_k,g}^{pp}\right\}$ can be calculated as $E\left\{SINR_{l_k,g}^{pp}\right\} = \frac{A{d_{l_k}}^{-\alpha}\lambda^{-1}}{B+CDE\left({d_{l_{k'},l_k}}^{-\alpha}\right)\lambda^{-1}}$, with $d_{l_{k'},l_k} \sim U\left(d_{pl}^{\min}, d_{RSU}\right)$, $A = C = p^{mul}\rho$, $B = \sigma^2$, and $D = \sum_{k'=1,k'\neq k}^{K_m}\sum_{l_{k'}=1}^{L_{k'}}\delta_{l_{k'}}[g]$. Similarly, the lower bound of p_{ml}^{pre} and p_{ml}^{com} can also be calculated with $d_{l,l_k} \sim U\left(d_v^{\min}, d_{pl}\right)$. $d_{pl}^{\min}$ is the shortest distance between platoons, d_{RSU} is the coverage of the RSU, $d_v^{\min}$ is the shortest distance between vehicles, and d_{pl} is the length of the platoon.

References

[1] J. Wang, J. Liu, and N. Kato, "Networking and Communications in Autonomous Driving: A Survey," *IEEE Commun. Surveys Tuts.*, vol. 21, no. 2, pp. 1243–1274, 2019.

[2] L. Jiang, J. Kheyrollahi, C. R. Koch *et al.*, "Cooperative truck platooning trial on Canadian public highway under commercial operation in winter driving conditions," *Proc. Inst. Mech. Eng. D*, 2024. [Online]. Available: https://doi.org/10.1177/09544070241245477

[3] M. Makridis, K. Mattas, A. Anesiadou *et al.*, "OpenACC. An open database of car-following experiments to study the properties of commercial ACC systems," *Transp. Res. Part C Emerg. Technol.*, vol. 125, p. 103047, 2021.

[4] K. Xiong, Z. Wang, S. Leng, and J. He, "A Digital-Twin-Empowered Lightweight Model-Sharing Scheme for Multirobot Systems," *IEEE Internet Things J.*, vol. 10, no. 19, pp. 17 231–17 242, 2023.

[5] V. Lesch, M. Breitbach, M. Segata *et al.*, "An Overview on Approaches for Coordination of Platoons," *IEEE Trans. Intell. Transp. Syst.*, vol. 23, no. 8, pp. 10 049–10 065, 2022.

[6] H. Li, T. Zhang, S. Zheng *et al.*, "Distributed MPC for Multi-Vehicle Cooperative Control Considering the Surrounding Vehicle Personality," *IEEE Trans. Intell. Transp. Syst.*, vol. 25, no. 3, pp. 2814–2826, 2024.

[7] J. Clancy, D. Mullins, B. Deegan *et al.*, "Wireless Access for V2X Communications: Research, Challenges and Opportunities," *IEEE Commun. Surveys Tuts.*, vol. 26, no. 3, pp. 2082–2119, 2024.

[8] Z. Tang, J. He, K. Yang *et al.*, "Matching 5G Connected Vehicles to Sensed Vehicles for Safe Cooperative Autonomous Driving," *IEEE Netw.*, vol. 38, no. 3, pp. 227–235, 2024.

[9] K. Xiong, S. Leng, C. Huang *et al.*, "Intelligent task offloading for heterogeneous v2x communications," *IEEE Trans. Intell. Transp. Syst.*, vol. 22, no. 4, pp. 2226–2238, 2021.

[10] L. Zhang, H. Xu, O. Onireti, M. A. Imran, and B. Cao, "How Much Communication Resource is Needed to Run a Wireless Blockchain Network?" *IEEE Netw.*, vol. 36, no. 1, pp. 128–135, 2022.

[11] H. Lee, H. Seo, and W. Choi, "Fast and Scalable Distributed Consensus Over Wireless Large-Scale Internet of Things Network," *IEEE Internet Things J.*, vol. 9, no. 11, pp. 7916–7930, 2022.

[12] H. Zhang, S. Leng, H. Yin, and S. Yu, "Intelligent Consensus Enhanced Spectrum Sharing in Heterogeneous Wireless Networks," *IEEE Internet Things J.*, pp. 1–1, 2024, early access, doi: 10.1109/JIOT.2024.3415622.

[13] D. Ongaro and J. Ousterhout, "In search of an understandable consensus algorithm," in *USENIX ATC 14*, 2014, pp. 305–319.

[14] M. Castro, B. Liskov *et al.*, "Practical byzantine fault tolerance," in *OsDI*, vol. 99, 1999, pp. 173–186.

[15] D. Yu, W. Li, H. Xu, and L. Zhang, "Low Reliable and Low Latency Communications for Mission Critical Distributed Industrial Internet of Things," *IEEE Commun. Lett.*, vol. 25, no. 1, pp. 313–317, 2021.

[16] 3GPP, "TS 23. 501: Technical specification group services and system aspects, system architecture for the 5G system (5GS)," *Release-17*, vol. v17.6.0, 2022.

[17] M. Won, "L-Platooning: A Protocol for Managing a Long Platoon With DSRC," *IEEE Trans. Intell. Transp. Syst.*, vol. 23, no. 6, pp. 5777–5790, 2022.

[18] S. B. Prathiba, G. Raja, K. Dev *et al.*, "A Hybrid Deep Reinforcement Learning For Autonomous Vehicles Smart-Platooning," *IEEE Trans. Veh. Technol.*, vol. 70, no. 12, pp. 13 340–13 350, 2021.

[19] K. Li, J. Wang, and Y. Zheng, "Cooperative Formation of Autonomous Vehicles in Mixed Traffic Flow: Beyond Platooning," *IEEE Trans. Intell. Transp. Syst.*, vol. 23, no. 9, pp. 15 951–15 966, 2022.

[20] C. Chen, Y. Zhang, M. R. Khosravi, Q. Pei, and S. Wan, "An Intelligent Platooning Algorithm for Sustainable Transportation Systems in Smart Cities," *IEEE Sens. J.*, vol. 21, no. 14, pp. 15 437–15 447, 2021.

[21] C. Feng, Z. Xu, X. Zhu *et al.*, "Wireless Distributed Consensus in Vehicle to Vehicle Networks for Autonomous Driving," *IEEE Trans. Veh. Technol.*, vol. 72, no. 6, pp. 8061–8073, 2023.

[22] H. Xu, Y. Fan, W. Li *et al.*, "Wireless Distributed Consensus for Connected Autonomous Systems," *IEEE Internet Things J.*, vol. 10, no. 9, pp. 7786–7799, 2023.

[23] H. Seo, J. Park, M. Bennis, and W. Choi, "Communication and Consensus Co-Design for Distributed, Low-Latency, and Reliable Wireless Systems," *IEEE Internet Things J.*, vol. 8, no. 1, pp. 129–143, 2021.

[24] M. K. Atiq, R. Muzaffar, Ó. Seijo, I. Val, and H.-P. Bernhard, "When IEEE 802.11 and 5G Meet Time-Sensitive Networking," *IEEE Open J. Ind. Electron. Soc.*, vol. 3, pp. 14–36, 2022.

[25] G. ACIA, "Integration of 5G with Time-Sensitive Networking for Industrial Communications," 2021.

[26] P. M. Rost and T. Kolding, "Performance of Integrated 3GPP 5G and IEEE TSN Networks," *IEEE Commun. Stand. Mag.*, vol. 6, no. 2, pp. 51–56, 2022.

[27] Y. Zhang, Q. Xu, M. Li *et al.*, "QoS-Aware Mapping and Scheduling for Virtual Network Functions in Industrial 5G-TSN Network," in *2021 GLOBECOM*, 2021, pp. 1–6.

[28] D. Wang and T. Sun, "Leveraging 5G TSN in V2X Communication for Cloud Vehicle," in *IEEE EDGE*, 2020, pp. 106–110.

[29] S. Boyd and A. Mutapcic, "Subgradient Methods," *Lecture notes of EE364b*, Stanford University, 2007.

[30] Y. Zheng, S. Wang, S. Yin, B. Wu, and Y. Liu, "Mix-Flow Scheduling for Concurrent Multipath Transmission in Time-Sensitive Networking," in *ICC Workshops 2021*, 2021, pp. 1–6.

[31] Y. Chen, Y. Wang, J. Zhang *et al.*, "QoS-Driven Spectrum Sharing for Reconfigurable Intelligent Surfaces (RISs) Aided Vehicular Networks," *IEEE Trans. Wireless Commun.*, vol. 20, no. 9, pp. 5969–5985, 2021.

[32] A. Liu, V. K. N. Lau, and B. Kananian, "Stochastic Successive Convex Approximation for Non-Convex Constrained Stochastic Optimization," *IEEE Trans. Signal Process.*, vol. 67, no. 16, pp. 4189–4203, 2019.

Jiayu Cao is currently pursuing the Ph.D. degree with the School of Information and Communication Engineering, University of Electronic Science and Technology of China (UESTC).

Her research interests include vehicular networks, autonomous driving, distributed consensus, mobile edge computing, and multi-agent systems.

Supeng Leng (Member, IEEE) received the Ph.D. degree from Nanyang Technological University (NTU), Singapore, in 2005.

He is a Full Professor with the School of Information and Communication Engineering, UESTC, China, and also with the Shenzhen Institute for Advanced Study, UESTC, Shenzhen, China. He is also the Director of the Sichuan International Joint Research Center on Ubiquitous Wireless Networks. He has been working as a Research Fellow with the Network Technology Research Center, NTU. He published over 200 research papers and four books/book chapters in recent years. His research focuses on resource, spectrum, energy, routing, and networking in Internet of Things, vehicular networks, broadband wireless access networks, and next generation intelligent mobile networks.

Prof. Leng received the Best Paper Awards at five IEEE international conferences. He serves as an organizing committee chair and a TPC member for many international conferences, as well as an Associate Editor for three international research journals, such as IEEE Internet of Things Journal.

Jianhua He (Senior Member, IEEE), received the Ph.D. degree from Nanyang Technological University, Singapore, in 2002.

He is currently a Professor with the University of Essex, Colchester, U.K. He published more than 150 research papers in refereed international journals and conferences. His main research interests include 5G/6G wireless communications and networks, connected vehicles, autonomous driving, Internet of Things, mobile edge computing, data analytics, AI, and machine learning.

Prof. He is the Workshop Chair of MobiArch'20 and ICAV'21 and a member of Editorial Board for several international journals. He is the Coordinator of EU Horizon2020 projects COSAFE and VESAFE and Horizon EU project SECOM on cooperative connected autonomous vehicles.

Hanwen Zhang received the Ph.D. degree from the University of Electronic Science and Technology of China (UESTC), Chengdu, China, in 2023. She is a Postdoctoral Researcher with UESTC, Chengdu.

Her research interests include spectrum sharing, internet of thing and blockchain.